# Preliminary study on simultaneous adsorption of nitrate and phosphate using $CaFe_2O_4$-modified biochar originated from lychee peels

**Lan Huong Nguyen*, Tuan Hiep Tran**

*Ho Chi Minh City University of Industry and Trade (HUIT), 140 Le Trong Tan Street, Tay Thanh Ward, Tan Phu District, Ho Chi Minh City, Vietnam*

Received 20 October 2023; revised 20 November 2023; accepted 22 January 2024

***Abstract:***

**In this study, lychee peels derived-biochar modified with $CaFe_2O_4$NPs (MLPB) were successfully fabricated to adsorb simultaneously both nitrate ($NO_3^-$) and phosphate ($PO_4^{3-}$) from aqueous solution. The preliminary investigation on the effect of operational parameters, including pyrolysis temperature and modification ratio on adsorption of nitrate ($NO_3^-$) and phosphate ($PO_4^{3-}$) in single-component and bi-component systems was performed. The characteristics of biochar (PLPB) and magnetic modified biochar (MLPB) were evaluated through the specific surface area, SEM, EDS and mapping, FTIR, and XRD. The primary results showed the adsorption of $NO_3^-$ and $PO_4^{3-}$ onto PLPB reached a peak at the pyrolysis temperature of 450°C with a $NO_3^-$ and $PO_4^{3-}$ adsorption capacity of 12.8 and 10.9 mg/g, respectively, in the single-component system while the adsorption capacity of $NO_3^-$ and $PO_4^{3-}$ in the bi-component system was 12.5 and 10.6 mg/g, respectively. The removal efficiency of $NO_3^-$ and $PO_4^{3-}$ maximised at a modification ratio of 5%. At this modification ratio, the adsorption capacity of $NO_3^-$ and $PO_4^{3-}$ in the single-component reached, respectively, 24.0 and 21.5 mg/g while the adsorption of $NO_3^-$ and $PO_4^{3-}$ was 24.0 and 22.6 mg/g in the bi-component system, respectively. The preliminary study on analysing characteristics of the adsorbent confirmed that the removal of $NO_3^-$ and $PO_4^{3-}$ was through ligand exchange and surface complexation mechanisms. The findings indicated that the MLPB was a feasible and fully promising adsorbent in the simultaneous removal of $NO_3^-$ and $PO_4^{3-}$ from the aqueous solution.**

***Keywords:*** **calcium spinel ferrites, lychee peel biochar, magnetic modified biochar, nitrate, phosphate.**

***Classification numbers:*** **2.2, 5.3**

## 1. Introduction

In recent years, with the massive growth of industry and agriculture, contamination of receiving water bodies by the excessive discharge of nitrate ($NO_3^-$) and phosphate ($PO_4^{3-}$) has become a vital issue worldwide. $NO_3^-$ and $PO_4^{3-}$ primarily originate from fertiliser residues in crop growth [1] and effluents from industries such as seafood processing and fertiliser production. Water bodies receiving excessive amounts of both $NO_3^-$ and $PO_4^{3-}$ simultaneously trigger eutrophication with algal blooms, leading to the depletion of dissolved oxygen in water, impairment of the self-cleaning capacity of receiving sources, and the death of aquatic organisms [1, 2]. Additionally, nitrate-contaminated drinking water can cause serious diseases such as methemoglobinemia, cancer, and blue baby syndrome [1, 3]. Therefore, it is essential to simultaneously remove both $NO_3^-$ and $PO_4^{3-}$ from wastewater before discharging into water bodies.

Techniques for removing $NO_3^-$ and $PO_4^{3-}$ include biological processes using microalgae *Chlorella vulgaris* [4] and pilot-scale SBR for nitrate removal [5], ion exchange [6, 7], chemical precipitation [8, 9], and adsorption [10, 11]. However, biological processes and chemical precipitation are not suitable for removing $NO_3^-$ and $PO_4^{3-}$ at very low concentrations and require a long biomass residence time [1]. In comparison, adsorption is considered a simple, low-cost, and highly efficient technique for removing $NO_3^-$ and $PO_4^{3-}$ at trace concentrations [1-3, 11].

Biochar is a product of the pyrolysis process of carbon-based materials, which has garnered more attention in the treatment of various pollutants, such as nitrate and phosphate. Especially, biochar derived from agro-industrial by-products has encouraged product development towards circular economic practices. Additionally, the utilisation of solid waste to fabricate biochar helps effectively manage solid waste and generate useful materials for pollutant removal from wastewater. To date, a large amount of agro-

*Corresponding author: Email: huongnl@huit.edu.vn

industrial by-products has been used to produce biochar for treating both $NO_3^-$ and $PO_4^{3-}$ from wastewater, such as biochar from sugarcane bagasse for $NO_3^-$ adsorption [2]; MgO-modified magnetic biochar derived from anaerobic digestion residue for $PO_4^{3-}$ removal [12]; Gigantochloa bamboo-derived biochar [13]; Copper modified activated bamboo charcoal for adsorption of trace metals and ruthenium dye wastes [14, 15], and activated carbon originated from musk-melon peel composited with $ZnFe_2O_4$ for simultaneous adsorption of both $NO_3^-$ and $PO_4^{3-}$ from wastewater [16]. Lychee peels are grown popularly in the Northern of Vietnam with an average yield of 40,000 tons/year [17]. The amount of lychee peel discharged makes up about 15% of the fresh weight of lychee. Besides, lychee peel has main components of cellulose, lignin which are suitable as potential carbon biomass for producing biochar [18].

However, the main drawback of applying agro-industrial by-products-derived biochars for pollutant removal is their low adsorption capacity towards pollutants due to their low specific surface area and inherent negatively charged surface. Thus, the biochar needs to be modified by chemical-physical methods to enhance pollutant adsorption capacity and efficiency. Among modification methods, loading spinel ferrite nanoparticles ($MFe_2O_4$) has proven to be highly efficient and overcome some limitations of biochars by increasing specific surface area ($S_{BET}$), well-developing a porous structure, and decreasing nanoparticle agglomeration. Specifically, L. Ma, et al. (2018) [8] reported magnesium ferrite ($MgFe_2O_4$)/biochar magnetic composites (MFB-MCs) exhibited superior $PO_4^{3-}$ adsorption capacity over biochar due to enlarged porosity along with increased available binding sites; adsorption of Cr(VI) onto $MnFe_2O_4$ reached a high value of 89.18 mg/g [19]; simultaneous removal of $NO_3^-$ and $PO_4^{3-}$ from wastewater by biochar/$ZnFe_2O_4$ composite achieved excellent adsorption capacities of 75.58 and 91.80 mg/g, respectively.

In the present work, lychee peels-originated biochar modified by spinel ferrite nanoparticles ($CaFe_2O_4$) was primarily studied for the simultaneous adsorption of both $NO_3^-$ and $PO_4^{3-}$ from wastewater in batch-mode tests. The primary study aims to investigate the effect of operational parameters, consisting of pyrolysis temperature, modification ratios between biochar and $CaFe_2O_4$ NPs on the simultaneous adsorption capacity and efficiency of $NO_3^-$ and $PO_4^{3-}$ from wastewater. Physical-chemical characteristics of biochar and modified biochar before and after loading both $NO_3^-$ and $PO_4^{3-}$ were determined using various analytical techniques such as nitrogen adsorption-desorption, scanning electron microscope (SEM), Fourier transform infrared (FTIR), XRD, and EDS and mapping. Besides, the plausible mechanisms of $NO_3^-$ and $PO_4^{3-}$ adsorption onto modified biochar were briefly discussed.

## 2. Materials and methods

### *2.1. Chemicals and materials*

The chemicals used for experiments, including $KH_2PO_4$, $NaNO_3$, KOH, $CaCl_2$, $FeCl_3$, glycerol, HCl and citric acid, were purchased from Kyamata (Japan). All chemicals were of analytical grade. Lychee peels were obtained from Bac Giang province, Vietnam.

The simulated wastewater containing $NO_3^-$ and $PO_4^{3-}$ was prepared by dissolving precisely 4.387 g $KH_2PO_4$ and 6.071 g $NaNO_3$ in 1000 ml double distilled water (DDW) separately to reach a stock solution of 1000 mg/l. The experimental solution was prepared by diluting the stock solution to the desired concentrations.

### *2.2. Preparation of biochars*

#### *2.2.1. Fabrication of biochar (PLPB)*

After collection, the lychee peels (LPs) were repeatedly washed using distilled water to remove all impurities attached to the LP's surface. Then, the LPs were exposed under sunlight. The dried LPs were then blended using blender and sieved to achieve a diameter of 60 µm. The blended LPs were impregnated in KOH 0.1 M by a homogeniser agitator to enrich oxygen-containing functional groups. The KOH-soaked LP was then filtered and repeatedly cleaned by DDW until pH reached 7.0. The LP was continuously dried at 105°C for many hours to obtain the dried LP powder. The dried LP powder was continuously pyrolysed in temperature ranges from 300-550°C (interval=50°C) with a heating rate of 10°C for 2 h. Finally, the obtained black solid was denoted as lychee peel-derived biochar (PLPB). The biochars obtained by pyrolysing at various temperatures were used for the next experiments to determine the optimal pyrolysis temperature for the fabrication of biochar, which was then used to modify with $CaFe_2O_4$ NPs in the following steps. The scheme describing the fabrication procedure of biochar from lychee peels was demonstrated in Fig. 1A.

#### *2.2.2. Fabrication of $CaFe_2O_4$NPs*

The spinel ferrite $CaFe_2O_4$ nanoparticles were formed using the sol-gel method as described in our previous study [3]. Briefly, the procedure for the fabrication of $CaFe_2O_4$NPs can be described as follows: firstly, a 500 ml beaker containing 100 ml DDW, and 93 g of citric acid was homogenised and placed on a magnetic agitator at 120 rpm, 60°C for 15 min. Next, a certain amount of $CaCl_2$ and

$FeCl_3$ at a molar ratio of 0.0015:0.001 in ethylene glycol ($C_2H_6O_2$) was added to the above beaker. The mixture was then agitated at 120 rpm at 80°C to achieve a completely dissolved solution. The mixture was then dried continuously at 105°C for 12 h to form a gel form. The gel was then calcined at 300°C for 3 h and further calcined at 1000°C for the next 2 h. Finally, the obtained black solid was $CaFe_2O_4$ NPs.

*2.2.3. The modification procedure of biochar with $CaFe_2O_4$ NPs*

The biochar was modified with $CaFe_2O_4$NPs using the wet impregnation method. In the first step of the procedure, a certain amount of $CaFe_2O_4$NPs at ratios of 1, 3, 5, 7, and 9% (w/w) was added into a certain volume of methanol in a 500 ml beaker. The beaker was then sonicated at 80°C for 30 min. Next, a certain amount of biochar (PLPB) was also added to the above beakers. The beakers were then stirred at 120 rpm for 2 h to ensure all $CaFe_2O_4$NPs were loaded onto the biochar's surface. The mixture was then centrifuged to collect the solid part. The obtained solid was cleaned with DDW and dried at 105°C for 2 h. The resulting product was magnetic modified biochar and labelled as MLPB-1; MLPB-3; MLPB-5; MLPB-7 and MLPB-9. Together with biochar (PLPB), the biochars at various modification ratios were used for simultaneous adsorption experiments of both $NO_3^-$ and $PO_4^{3-}$ to choose the optimal modification ratio.

### 2.3. Adsorption experiment design

All adsorption tests were conducted in batch-mode using Erlenmeyer flasks containing 100 ml $NO_3^-$ and $PO_4^{3-}$ (50 mg/l for each ion), 0.4 g of adsorbent with agitation at 150 rpm at room temperature (25±2°C) for 3 h of reaction time. All tests were performed in triplicate. The experimental data were expressed as the average value ± standard deviation. The adsorption capacity and performance of $NO_3^-$ and $PO_4^{3-}$ onto biochars were calculated using the following equations:

$$q = \frac{(C_o - C_e)V}{M} \quad (1)$$

$$\%H = \frac{(C_o - C_e)}{C_o} x100\% \quad (2)$$

where $q$ (mg/g) and $\%H$ are the adsorption capacity and efficiency of nitrate and phosphate onto biochars, respectively; $C_o$ and $C_e$ are concentrations of $NO_3^-$ and $PO_4^{3-}$ (mg/l) at initial and equilibrium, respectively; $V$ is the solution volume (l); and $M$ is the mass of applied biochar (g).

### 2.4. Analysis method

The physical-chemical characteristics of adsorbents before and after the adsorption process were determined. Specifically, the nitrogen adsorption-desorption isotherm was applied to measure the textural properties of materials at 77 K using Quantachrome Instruments version NOVA4000e. A D8 Phaser X-ray diffractometer was used to analyse the crystalline phase structure of adsorbents with a scanning angle of 10-80°. The surface morphology was observed by a scanning electron microscope (SEM). The elements' distribution on the adsorbents was evaluated via energy-dispersive X-ray spectroscopy (EDS) and mapping using S-4800, Hitachi, Japan.

The residual $NO_3^-$ and $PO_4^{3-}$ concentrations in the solution were measured according to the standard method [20] by spectrophotometric method using Spectrophotometer photoLab®7600 UV-VIS (WTW, Germany). The $NO_3^-$ was analysed according to 4500-$NO_3^-$ - nitrogen at λ=415 nm with sulfosalicylic acid. The $PO_4^{3-}$ was measured according to 4500 P-B&E using ammonium molybdate at λ=880 nm. Measurement of $NO_3^-$ was based determination of the UV-Vis absorption spectrum of the yellow compound formed by the reaction of 10 g/l sulfosalicylic acid (formed by adding sodium salicylate and sulfuric acid to the test sample) with nitrate and subsequent treatment with alkali. Afterwards, measure the absorbance of the solution at 415 nm. Meanwhile, the phosphate was determined by Ascorbic Acid Method, 4500 P-B&E, Standard Methods for the Examination of Water and Wastewater 23rd edition. In this procedure, ammonium molybdate and potassium antimonyl tartrate react in acid medium with orthophosphate to form a heteropoly acid-phosphomolybdic acid that is reduced to intensely coloured molybdenum blue by ascorbic acid. Afterwards, measure the absorbance of the solution at 880 nm. The pH meter (HANNA, pH HI 2002-02, Romani, American) was used to determine solution pH values.

## 3. Results and discussion

### 3.1. Effect of pyrolysis temperature on the adsorption of $NO_3^-$ and $PO_4^{3-}$

The tests to evaluate the effect of pyrolysis temperature on the adsorption of $NO_3^-$ and $PO_4^{3-}$ in the single-system and bi-component system were conducted with fixing initial concentrations of $NO_3^-$ and $PO_4^{3-}$ at 50 mg/l, adsorbent dosage of 4.0 g/l with varying pyrolysis temperatures in the range from 300-550°C. The $NO_3^-$ and $PO_4^{3-}$ adsorption capacities on the biochar at different pyrolysis temperatures in both single- and bi-component systems are illustrated in Fig. 1.

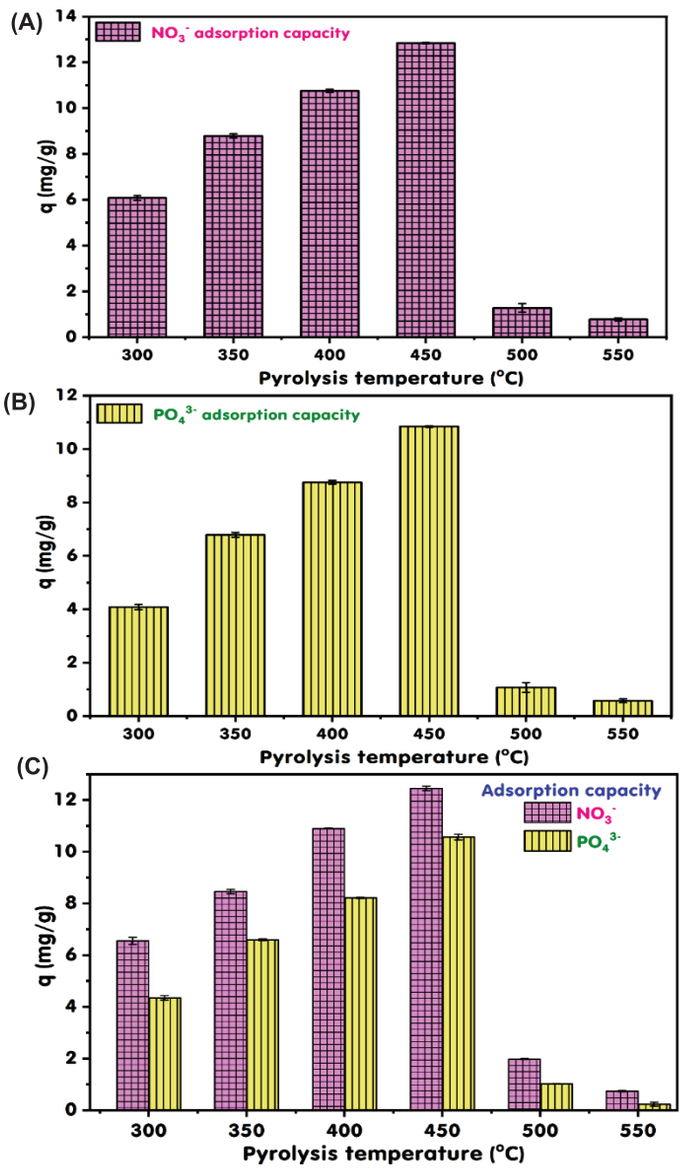


**Fig. 1. Effect of pyrolysis temperature on $NO_3^-$ and $PO_4^{3-}$ by (A, B) single-component and (C) bi-component systems.** Experimental conditions: $NO_3^-$ and $PO_4^{3-}$ (50 mg/l for each ion), 0.4 g of adsorbent, pH of 7.0 with varying of pyrolysis temperatures from 300-500°C.

The data in Fig. 1 demonstrate that the adsorption of $NO_3^-$ and $PO_4^{3-}$ strongly depended on the pyrolysis temperature [21, 22] in both single- and bi-component systems, and there was no significant difference in $NO_3^-$ and $PO_4^{3-}$ adsorption capacity in the single-component system and bi-component system. The $NO_3^-$ and $PO_4^{3-}$ adsorption capacities increased when the pyrolysis temperature rose. The $NO_3^-$ and $PO_4^{3-}$ adsorption capacity increased, respectively, from 6.08 to 12.84 mg/g and from 4.08 to 10.84 mg/g in the single-component system (Figs. 1A and 1B) and from 6.56 to 12.45 mg/g and from 4.36 to 10.57 mg/g in the bi-component system when the pyrolysis temperature was raised from 300-450°C. The $NO_3^-$ and $PO_4^{3-}$ adsorption maximised at a pyrolysis temperature of 450°C with an adsorption capacity of 12.84 and 10.84 mg/g, respectively, in the single-component system and 12.45 and 10.57 mg/g, respectively, in the bi-component system. However, a further increase in pyrolysis temperature from 500-550°C led to a strong drop in $NO_3^-$ and $PO_4^{3-}$ adsorption capacity on the biochar. The results were because a very low or very high temperature is not favourable for the production of biochar because samples seem to have turned into ash. A very low temperature causes incomplete pyrolysis of carbon constituent in the material while a very high temperature leads to ashing of the carbon composition in the material, thus the adsorption capacity was decreased [23]. The highest adsorption capacity of $NO_3^-$ and $PO_4^{3-}$ at a pyrolysis temperature of 450°C was due to a well-development in porous property and $S_{BET}$ of biochar at a suitable pyrolysis temperature [21, 24]. Therefore, the optimal pyrolysis temperature for the fabrication of biochar was chosen as 450°C in this work. Fig. 2 demonstrated biochar product images were produced at various pyrolysis temperatures.

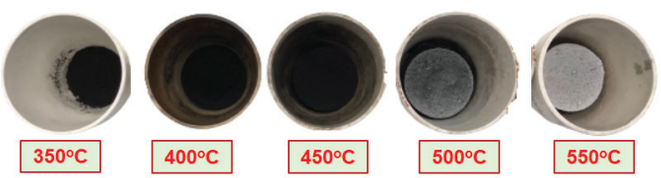


**Fig. 2. Images of the biochar products obtained at different pyrolysis temperatures.**

### *3.2. Effect of modification ratio on $NO_3^-$ and $PO_4^{3-}$ adsorption in the single-component and bi-component systems*

In this test, the lychee peels-derived biochar pyrolysed at 450°C was used to modify with $CaFe_2O_4$ NPs at various ratios of 0, 1, 3, 5, 7, and 9% (w/w) to promote $NO_3^-$ and $PO_4^{3-}$ adsorption capacity in both single-component and bi-component systems. The tests were performed by fixing initial concentrations of $NO_3^-$ and $PO_4^{3-}$ at 50 mg/l, biochar dosage of 4.0 g/l, and varying modification ratios of 0, 1, 3, 5, 7, and 9% (w/w) between biochar (PLPB) and $CaFe_2O_4$ NPs.

It can be seen from the data in Fig. 3 that the removal of both $NO_3^-$ and $PO_4^{3-}$ had a negligible difference in the single-component and bi-component systems, proving that there was no competition of binding sites for adsorption of these ions. When the amount of $CaFe_2O_4$NPs loaded on the biochar increased from 1 to 5%, the $NO_3^-$ and $PO_4^{3-}$ adsorption capacity and performance onto modified biochar in both systems increased. Specifically, the adsorption capacity of $NO_3^-$ and $PO_4^{3-}$ increased from 13.79 to 24.05 mg/g and from 12.39 to 21.52 mg/g, respectively, in the single-component system. The $NO_3^-$ and $PO_4^{3-}$ adsorption

capacity in the bi-component system increased from 15.46 to 24.05 mg/g and from 14.60 to 22.57 mg/g, respectively, when the modification ratio increased from 1-5%. The adsorption capacity and performance of both $NO_3^-$ and $PO_4^{3-}$ reached a peak at a modification ratio of 5% in both single- and bi-component systems. At a modification ratio of 5%, the $NO_3^-$ adsorption capacity was 24.05 mg/g with a $NO_3^-$ removal efficiency of 95.36%, and the $PO_4^{3-}$ adsorption capacity reached 21.52 mg/g with a removal efficiency of 87.09% in the single system. Similarly, the $NO_3^-$ and $PO_4^{3-}$ adsorption capacities in the bi-component system reached 24.05 mg/g and 22.57 mg/g, respectively. The $NO_3^-$ and $PO_4^{3-}$ adsorption capacity in both single- and bi-component systems onto biochar was the lowest. The $NO_3^-$ and $PO_4^{3-}$ adsorption capacities onto modified biochar at a ratio of 5% were higher than that of biochar (PLPB) by many times.

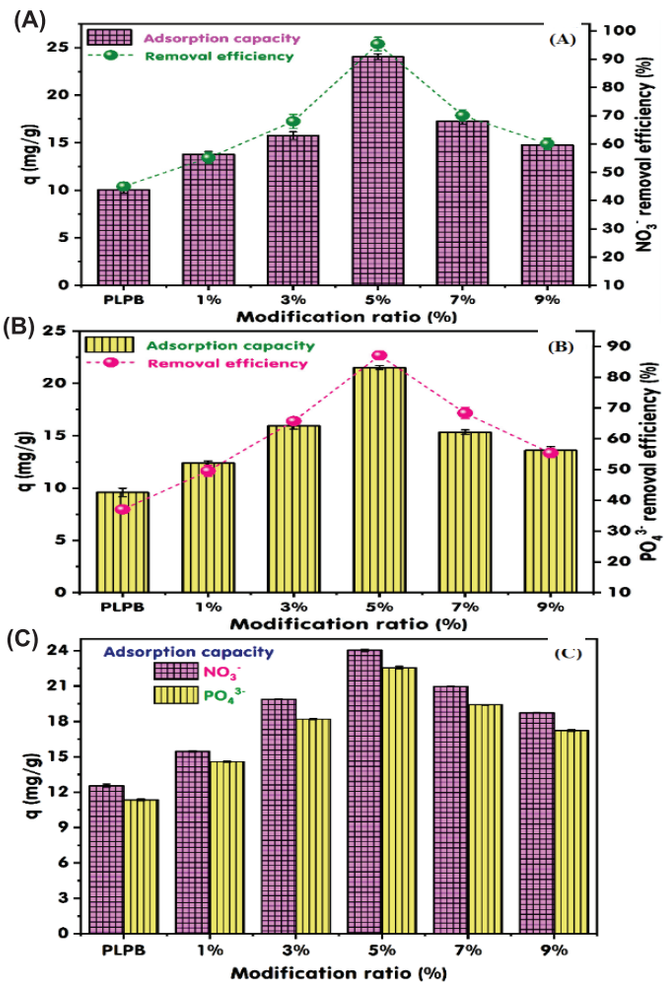


**Fig. 3. $NO_3^-$ and $PO_4^{3-}$ adsorption capacity and efficiency in the (A, B) single-component and (C) bi-component systems.** Experimental conditions: $NO_3^-$ and $PO_4^{3-}$ (50 mg/l for each ion), 0.4 g of adsorbent, pH of 7.0 with varying of modification ratios between biochar and $CaFe_2O_4$ from 1-9%.

However, a further growth in the loading ratio of nanoparticles onto biochar led to a moderate drop in $NO_3^-$ and $PO_4^{3-}$ adsorption capacity and efficiency in both single- and bi-component systems. The removal of $NO_3^-$ was 17.28 and 14.77 mg/g, which decreased by 6.77 and 9.30 mg/g, while removal of $PO_4^{3-}$ reached 15.34 and 13.59 mg/g, which dropped by 6.18 and 7.43 mg/g when the modification ratio increased from 5 to 7 and 9% in the single-component system. Meanwhile, the simultaneous adsorption of both $NO_3^-$ and $PO_4^{3-}$ in the bi-component system saw a similar trend. To be specific, the adsorption of $NO_3^-$ dropped by 3.07 and 5.33 mg/g, and $PO_4^{3-}$ adsorption fell by 3.14 and 5.33 mg/g when the modification ratio increased from 5 to 7 and 9%.

The results showed that there was an optimal modification ratio in which the $NO_3^-$ and $PO_4^{3-}$ adsorption capacity and efficiency in both single- and bi-component systems were the highest. A very low or very high loading ratio was not beneficial for the adsorption of $NO_3^-$ and $PO_4^{3-}$ onto biochar. A very low loading ratio of nanoparticles led to a lack of binding sites on the biochar's surface, while a very high loading ratio caused overlapping pores on the biochar's surface, thus the adsorption capacity was dropped. The similar results were also obtained by previous scholars. For instance, B. Wu, et al. (2017) [25] used magnetic $La(OH)_3/Fe_3O_4$ nanocomposites with varied La-to-Fe mass ratios of 1:1, 2:1, 4:1, and 5:1 for adsorption of $PO_4^{3-}$ and the result showed that La-to-Fe mass ratio of 4:1 had the highest removal efficiency of $PO_4^{3-}$. A low or high ratio of La was not favourable for adsorption of $PO_4^{3-}$. H.H.P. Quang, et al. (2022) [26] studied adsorption of $NO_3^-$ onto drinking water sludge (DWS) coated by $ZrO_2$ nanoparticles (DWS@$ZrO_2$) and results indicated that either low (0.05 M) or high $ZrO_2$ concentrations (0.3 and 0.5 M) had a negative effect on the $NO_3^-$ adsorption capacity. The $NO_3^-$ adsorption capacity maximised at coating $ZrO_2$ concentration of 0.1 M. This result was because the limited active sites on the surface of absorbents at low concentration of $ZrO_2$ caused a lack of adsorption sites for ion $NO_3$-, while a high $ZrO_2$ concentration led to negligible active adsorption sites on the surface of absorbents for nitrate adsorption, resulting in a drop in nitrate adsorption capacity. From the above discussions, a loading ratio of 5% $CaFe_2O_4$ NPs was selected to modify lychee peels-derived biochar for the adsorption promotion of both $NO_3^-$ and $PO_4^{3-}$ in single- and bi-component systems in this work.

### *3.3. Adsorbent characteristics and adsorption mechanism briefly discussion*

In this present work, the chemical-physical properties of biochar (PLPB) and modified biochar at the optimal ratio of 5% (MLPB-5) were assessed to briefly determine $NO_3^-$ and $PO_4^{3-}$ adsorption mechanisms in the bi-component system.

**Table 1. Nitrogen adsorption-desorption isotherm data of PLPB, MLPB-5 before adsorption, PLPB; MLPB-5 after adsorption in bi-component system.**

| | | Before adsorption | | After adsorption | |
|---|---|---|---|---|---|
| | *Unit* | *PLPB* | *MLPB-5* | *PLPB* | *MLPB-5* |
| $S_{BET}$ | $m^2/g$ | 1.554 | 2.618 | 0.616 | 1.183 |
| $V_{pore}$ | $cm^3/g$ | 0.006 | 0.007 | 0.004 | 0.005 |
| $D_{pore}$ | nm | 4.117 | 4.153 | 3.535 | 4.111 |

As can be seen from the data in Table 1, the biochar was modified by $CaFe_2O_4$ NPs, witnessing a growth in specific surface area by about 1.7 times. Moreover, the loading of $CaFe_2O_4$ NPs also led to a well-developed porous structure of the modified biochar. This result was due to the occurrence of both Ca and Fe on the modified biochar's surface. Similar results were also indicated in previous works. For example, the loading of $MgFe_2O_4$ onto biochar derived from *Undaria pinnatifida* roots for the adsorption of $PO_4^{3-}$ caused an increase in the $S_{BET}$ of the modified biochar (MFB-MCs) by 6.12 times [27]. The $S_{BET}$ of $ZrO_2$-modified biochar also increased by 2.81 times compared with biochar [26]. After the adsorption of both $NO_3^-$ and $PO_4^{3-}$ in the bi-component system, the $S_{BET}$ of $NO_3^-$ and $PO_4^{3-}$-laden PLPB and $NO_3^-$ and $PO_4^{3-}$-laden MLPB-5 decreased due to filling porous holes on the biochar's surface by several $NO_3^-$ and $PO_4^{3-}$ ions. Similar results were also reported by previous research [1, 25, 26].

However, the $S_{BET}$ data of biochars in Table 1 also indicated that both PLPB and MLPB-5 belong to non-porous material with a low $S_{BET}$. Thus, the $NO_3^-$ and $PO_4^{3-}$ adsorption by pore-filling mechanism was negligible in this study.

The surface morphology of PLPB and MLPB-5 before and after simultaneous adsorption of $NO_3^-$ and $PO_4^{3-}$ in the bi-component system are presented in Fig. 4.

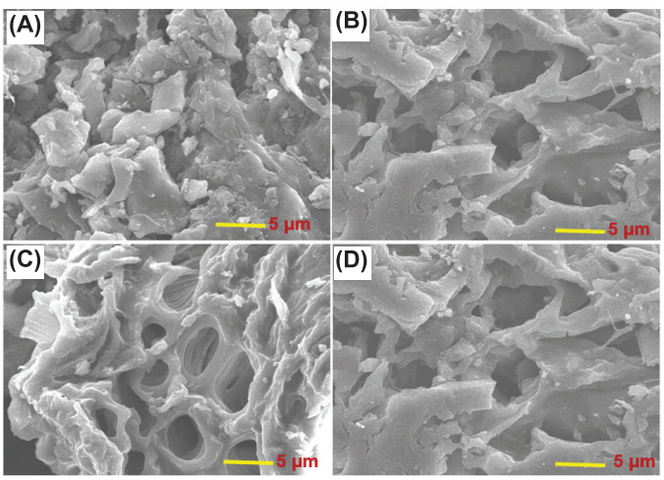


**Fig. 4. SEM images of (A) PLPB and (C) MLPB-5 before adsorption; (B) PLPB and (D) MLPB-5 after adsorption in a bi-component system.**

From Fig. 4A, it is evident that the PLPB before adsorption had a heterogeneous surface with a rough structure. Several tiny fine pores were observed in the SEM image of MLPB-5 before adsorption, confirming that there was an amount of $CaFe_2O_4$ NPs stacked onto the porous surface of biochar in the form of irregular flakes (Fig. 4C). Fig. 4C also showed MLPB-5 had a porous structure with several scroll layers on the surface. After adsorption, the porous structure on both PLPB and MLPB-5 was broken and blocked with $NO_3^-$ and $PO_4^{3-}$ ions. The result suggested that the $Ca^{2+}$ and $Fe^{2+}$ on the biochar's surface reacted with nitrate and phosphate through chemical or physical adsorption [2].

Based on EDS analysis results (Fig. 5), the biochar contained C, O, Mg, S, K and Ca in its constituent (Fig. 5A). After being loaded by $CaFe_{2O4}$ NPs, there was an occurrence of Ca and Fe with a high amount in the modified biochar composition, proving that the $CaFe_2O_4$ NPs were successfully loaded on the biochar's surface (Fig. 5C).

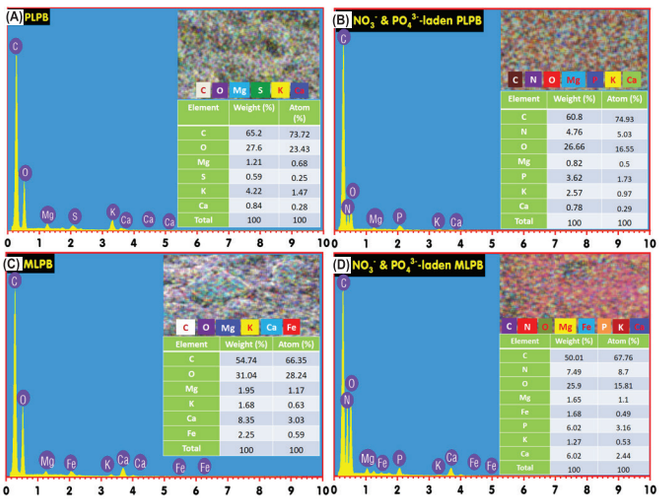


**Fig. 5. EDS spectrums and elements mapping of (A) PLPB and (C) MLPB-5 before adsorption; and (B) PLPB and (D) MLPB-5 after adsorption in a bi-component system.**

Especially, after adsorption, both N and P were present in the biochars' constituent, confirming that both $NO_3^-$ and $PO_4^{3-}$ ions were successfully adsorbed by PLPB and MLPB-5. With the same initial concentration of pollutants, the adsorbed amount of N and P on the MLPB-5 was higher than that of the PLPB by about 2 times, indicating that the $NO_3^-$ and $PO_4^{3-}$ adsorption capacity on the modified biochar was higher than that of biochar.

The XRD patterns of biochar and modified biochar before and after $NO_3^-$ and $PO_4^{3-}$ adsorption in the bi-component system are demonstrated in Fig. 6A. The successful loading of both Ca and Fe on MLPB-5's surface was also confirmed by the XRD pattern (Fig. 6A). As indicated in Fig. 6B, the biochar (PLPB) before and after adsorption exhibited an amorphous structure. This was also an inherent property of biochar

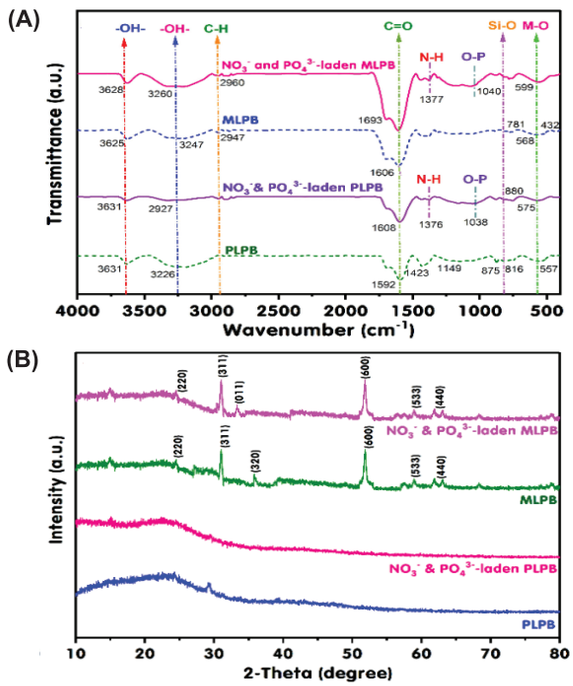


**Fig. 6. FTIR of PLPB and MLPB-5 (A) XRD of PLPB and (B) MLPB-5 in a bi-component system.**

produced from carbon-based materials. On the other hand, the $CaFe_2O_4$-modified biochar expressed a nanocrystalline structure both before and after adsorption with the appearance of typical characteristic peaks of $CaFe_2O_4$. All these typical peaks were well agreed with the standard $CaFe_2O_4$ spectra (JCPDS Card No. 74-2136) [3]. The 2θ values at 26.2°, 33.6°, 39.5°, 52.7°, 61.2°, and 67.7° corresponded with the typical crystal planes of calcium ferrite with good purity of $CaFe_2O_4$ at (220), (311), (320), (600), (533), and (440) planes, confirming that $CaFe_2O_4$ nanoparticles were successfully deposited on the PLPB's surface. In combination with data in Fig. 5 which demonstrated the distribution of Fe, Ca, O, N and P in the modified biochar constituent, leading to the formation of Fe-O-P, Ca-O-P, Fe-O-N and Ca-O-N complexes on the biochar's surface by covalent binding of nitrate and phosphate ions with –OH functional groups, confirming the surface complexation mechanism contributed to the removal of both $NO_3^-$ and $PO_4^{3-}$ by MPLP. The surface complexation mechanism was also confirmed by FTIR data (Fig. 6A) by the formation of complexes of P-O-M and N-H groups. Similar results were achieved by previous studies [26, 28].

The FTIR analysis revealed dense peaks density at 3228 and 3226 $cm^{-1}$ in biochars before adsorption, indicating the presence of –OH stretching and vibration of –OH groups [2, 26]. However, the density of –OH groups decreased in $NO_3^-$ and $PO_4^{3-}$-laden biochars, suggesting that the –OH groups participated in the adsorption process. Moreover, peaks fluctuating around 2947 and 2940 $cm^{-1}$ were attributed to C-H groups in biochar. The peaks density around 1592 and 1608 $cm^{-1}$ corresponded to C=O groups. Notably, the occurrence of new peaks at 1376 and 1377 $cm^{-1}$ after adsorption may indicate band vibration of O-N, while peaks at 1038 and 1040 $cm^{-1}$ were associated with N-H groups. This result confirmed chemical/physical interactions between the biochars' surface and $NO_3^-$ and $PO_4^{3-}$ during the adsorption process, demonstrating successful adsorption of both ions onto the biochars. Additionally, peaks vibrating around 781 $cm^{-1}$ to 880 $cm^{-1}$ were attributed to Si-O bonds. The bands at 432, 575, and 599 $cm^{-1}$ denoted the stretching vibration of M-O, P-O-M, and N-O-M (M=Fe, Ca), respectively. Analysis of the FTIR data indicated a ligand exchange reaction occurred between –OH groups on the surface-modified biochar and $NO_3^-$ and $PO_4^{3-}$ anions during the adsorption process. Thus, ligand exchange was identified as the main adsorption mechanism of $NO_3^-$ and $PO_4^{3-}$ anions onto modified biochar in the bi-component system.

In summary, based on the above-discussed physical-chemical characteristics of biochars, it can be concluded that the removal of both $NO_3^-$ and $PO_4^{3-}$ in the bi-component system occurred via surface complexation and ligand exchange mechanisms.

## 4. Conclusions

This study successfully developed a low-cost adsorbent from waste lychee peels and modified it with $CaFe_2O_4$ NPs for the removal of both $NO_3^-$ and $PO_4^{3-}$ from wastewater. The optimal pyrolysis temperature for fabricating biochar was determined to be 450°C. Furthermore, the results indicated that a modification ratio of 5% $CaFe_2O_4$ NPs with biochar provided the highest $NO_3^-$ and $PO_4^{3-}$ adsorption capacity and efficiency in both single- and bi-component systems, with negligible differences observed in the adsorption performance between the single-component and bi-component systems. The $NO_3^-$ and $PO_4^{3-}$ adsorption capacities onto MPLB were consistently higher than those onto PLPB, approximately double. Analysis of the physical-chemical properties data of biochars before and after adsorption primarily determined that the $NO_3^-$ and $PO_4^{3-}$ adsorption mechanisms were through surface complexation and ligand exchange. These findings suggest that $CaFe_2O_4$-modified biochar holds significant promise for the simultaneous removal of both $NO_3^-$ and $PO_4^{3-}$ from wastewater. Moreover, the spent adsorbent containing $NO_3^-$ and $PO_4^{3-}$ can be utilised as a slow fertiliser for plant growth.

## CRediT author statement

Lan Huong Nguyen: Supervision, Original draft preparation, Writing - Reviewing and Editing, Conceptualisation, Methodology, Software; Tuan Hiep Tran: Visualisation, Investigation, Data curation.

## COMPETING INTERESTS

The authors declare that there is no conflict of interest regarding the publication of this article.

## REFERENCES


[1] W. Yang, X. Shi, J. Wang, et al. (2019), "Fabrication of a novel bifunctional nanocomposite with improved selectivity for simultaneous nitrate and phosphate removal from water", *ACS Appl. Mater. Interfaces*, **11(38)**, pp.35277-35285, DOI: 10.1021/acsami.9b08826.

[2] L.D.H. Hafshejani, A. Hooshmand, A.A. Naseri, et al. (2016), "Removal of nitrate from aqueous solution by modified sugarcane bagasse biochar", *Ecol. Eng.*, **95**, pp.101-111, DOI: 10.1016/j.ecoleng.2016.06.035.

[3] M.T. Le, X.H. Nguyen, T.P. Nguyen, et al. (2023), "Lychee peels-derived biochar-supported $CaFe_2O_4$ magnetic nanocomposite as an excellent adsorbent for effective removal of nitrate and phosphate from wastewater", *J. Environ. Chem. Eng.*, **11(5)**, DOI: 10.1016/j.jece.2023.110991.

[4] M.B. Sabeti, M.A. Hejazi, A. Karimi (2019), "Enhanced removal of nitrate and phosphate from wastewater by *Chlorella vulgaris*: Multi-objective optimization and CFD simulation", *Chinese J. Chem. Eng.*, **27(3)**, pp.639-648, DOI: 10.1016/j.cjche.2018.05.010.

[5] D. Scaglione, G. Tornotti, A. Teli, et al. (2013), "Nitrification denitrification via nitrite in a pilot-scale SBR treating the liquid fraction of co-digested piggery/poultry manure and agro-wastes", *Chem. Eng. J.*, **228**, pp.935-943, DOI: 10.1016/j.cej.2013.05.075.

[6] S. Guida, G. Rubertelli, B. Jefferson, et al. (2021), "Demonstration of ion exchange technology for phosphorus removal and recovery from municipal wastewater", *Chem. Eng. J.*, **420**, DOI: 10.1016/j.cej.2021.129913.

[7] T.E. Bektaş, B.K. Ugŭrluoğlu, B. Tan (2021), "Phosphate removal by ion exchange in batch mode", *Water Pract. Technol.*, **16(4)**, pp.1343-1354, DOI: 10.2166/wpt.2021.072.

[8] L. Ma, S. Yuan, F. Ji, et al. (2018), "Ammonia and phosphorous precipitation through struvite crystallization from swine wastewater with high suspended solid", *Desalin. Water Treat.*, **116**, pp.258-266, DOI: 10.5004/dwt.2018.22589.

[9] M.M. Maroneze, L.Q. Zepka, J.G. Vieira, et al. (2014), "Phosphorus removal technology: Management of the element in industrial waste", *Rev. Ambient. Água.*, **9(3)**, pp.445-458, DOI: 10.4136/1980-993X (in Portuguese).

[10] H.A.T. Banu, P. Karthikeyan, S. Meenakshi (2021), "Removal of nitrate and phosphate ions from aqueous solution using zirconium encapsulated chitosan quaternized beads: Preparation, characterization and mechanistic performance", **3**, *Results in Surfaces and Interfaces*, DOI: 10.1016/j.rsurfi.2021.100010.

[11] A. Gizaw, F. Zewge, A. Kumar, et al. (2021), "A comprehensive review on nitrate and phosphate removal and recovery from aqueous solutions by adsorption", *Aqua Water Infrastructure, Ecosyst. Soc.*, **70(7)**, pp.921-947, DOI: 10.2166/aqua.2021.146.

[12] J. Liu, J. Jiang, A. Aihemaiti, et al. (2019), "Removal of phosphate from aqueous solution using MgO-modified magnetic biochar derived from anaerobic digestion residue", *J. Environ. Manage.*, **250**, DOI: 10.1016/j.jenvman.2019.109438.

[13] N. Suhaimi, M.R.R. Kooh, C.M. Lim, et al. (2022), "The use of *Gigantochloa* bamboo-derived biochar for the removal of methylene blue from aqueous solution", *Adsorpt. Sci. Technol.*, **2022**, pp.22-24, DOI: 10.1155/2022/8245797.

[14] A. Masanizan, C.M. Lim, M.R.R. Kooh, et al. (2021), "The removal of ruthenium-based complexes $N_3$ dye from DSSC wastewater using copper impregnated KOH-activated bamboo charcoal", *Water, Air, Soil Pollut.*, **232**, DOI: 10.1007/s11270-021-05333-7.

[15] R. Thotagamuge, M.R.R. Kooh, A.H. Mahadi, et al. (2021), "Copper modified activated bamboo charcoal to enhance adsorption of heavy metals from industrial wastewater", *Environ. Nanotechnology, Monit. Manag.*, **16**, DOI: 10.1016/j.enmm.2021.100562.

[16] P. Karthikeyan, P. Sirajudheen, M.R. Nikitha, et al. (2020), "Removal of phosphate and nitrate via a zinc ferrite@activated carbon hybrid composite under batch experiments: Study of isotherm and kinetic equilibriums", *Environ. Nanotechnology, Monit. Manag.*, **14**, DOI: 10.1016/j.enmm.2020.100378.

[17] M.K.V. Carr, C.M. Menzel (2014), "The water relations and irrigation requirements of lychee (*Litchi chinensis* Sonn.): A review", *Exp. Agric.*, **50(4)**, pp.481-497, DOI: 10.1017/S0014479713000653.

[18] J. Wu, J. Yang, P. Feng, et al. (2020), "High-efficiency removal of dyes from wastewater by fully recycling litchi peel biochar", *Chemosphere*, **246**, DOI: 10.1016/j.chemosphere.2019.125734.

[19] N. Sezgin, A. Yalçın, Y. Köseoğlu (2016), "$MnFe_2O_4$ nano spinels as potential sorbent for adsorption of chromium from industrial wastewater", *Desalin. Water Treat.*, **57(35)**, pp.16495-16506, DOI: 10.1080/19443994.2015.1088808.

[20] L. Bridgewater, American Public Health Association, American Water Works Association, et al. (2012), *Standard Methods for The Examination of Water and Wastewater*, American Public Health Association, 724pp.

[21] Y. Li, S. Ma, S. Xu, et al. (2020), "Novel magnetic biochar as an activator for peroxymonosulfate to degrade bisphenol A: Emphasizing the synergistic effect between graphitized structure and $CoFe_2O_4$", *Chem. Eng. J.*, **387**, DOI: 10.1016/j.cej.2020.124094.

[22] T.H. Nguyen, X.H. Nguyen, T.G. Do, et al. (2023), "Development of biochar supported $NiFe_2O_4$ composite for peroxydisulfate (PDS) activation to effectively remove moxifloxacin from wastewater", *Chem. Eng. J. Adv.*, **16**, DOI: 10.1016/j.ceja.2023.100550.

[23] J. He, Y. Xiao, J. Tang, et al. (2019), "Persulfate activation with sawdust biochar in aqueous solution by enhanced electron donor-transfer effect", *Sci. Total Environ.*, **690**, pp.768-777, DOI: 10.1016/j.scitotenv.2019.07.043.

[24] C. Zhao, B. Shao, M. Yan, et al. (2021), "Activation of peroxymonosulfate by biochar-based catalysts and applications in the degradation of organic contaminants: A review", *Chem. Eng. J.*, **416**, DOI: 10.1016/j.cej.2021.128829.

[25] B. Wu, L. Fang, J.D. Fortner, et al. (2017), "Highly efficient and selective phosphate removal from wastewater by magnetically recoverable $La(OH)_3/Fe_3O_4$ nanocomposites", *Water Res.*, **126**, pp.179-188, DOI: 10.1016/j.watres.2017.09.034.

[26] H.H.P. Quang, K.T. Phan, N.T. Dinh, et al. (2022), "Using $ZrO_2$ coated sludge from drinking water treatment plant as a novel adsorbent for nitrate removal from contaminated water", *Environ. Res.*, **212**, DOI: 10.1016/j.envres.2022.113410.

[27] K.W. Jung, S. Lee, Y.J. Lee (2017), "Synthesis of novel magnesium ferrite ($MgFe_2O_4$)/biochar magnetic composites and its adsorption behavior for phosphate in aqueous solutions", *Bioresour. Technol.*, **245**, pp.751-759, DOI: 10.1016/j.biortech.2017.09.035.

[28] M. Ahmad, M. Ahmad, A.R.A. Usman, et al. (2018), "Biochar composites with nano zerovalent iron and eggshell powder for nitrate removal from aqueous solution with coexisting chloride ions", *Environ. Sci. Pollut. Res.*, **25(26)**, pp.25757-25771, DOI: 10.1007/s11356-017-0125-9.